Implementation of Hybrid Energy Storage System (Battery/Super-Capacitor) in DC Micro grid

Voruganti Bharath kumar[1], P.Kamalakar[2], Dr. N. Ramchandra[3], G. Esha[4]

[1,2,4] *Assistant Professor in Department of Electrical and Electronics Engineering*

[3] *Professor in Department of Electrical and Electronics Engineering*

[1, 3, 4] *St. Martin's Engineering College, Secunderabad, Telangana, India*

[2] *Malla Reddy Engineering college, Secunderabad, Telangana, India*

[1] *vorugantieee@gmail.com,* [2] *kamaleee209@gmail.com,* [3] *ramceee@smec.ac.in,* [4] *geshaeee@smec.ac.in*

***Abstract*— Energy storage technology (EST) is an important way to boost the power output of renewable energy production (such as solar and wind energy), but it is difficult for a single energy storage device (ESS) to satisfy the demand for secure grid service. A battery / super-capacitor HESS is proposed according to the configuration and operating characteristics of the current battery / super-capacitor hybrid energy storage system (HESS). The HESS work theory and three working modes (the super-capacitor pre-loading cold stand-by mode, boost mode and buck mode) are studied in detail. The boost mode and buck mode state equations are extracted. To create the small signal equivalent model under the buck / boost mode, the state space average method is used. In addition, the HESS charge and discharge control technique is obtained via the combination of the closed-loop voltage control. In Matlab / Simulink, the simulation model is designed to verify the efficacy of the suggested HESS and its control strategy. The results show that the HESS and its control strategy can ensure good stability and superior anti-interference of the DC bus voltage, and can simultaneously produce large current, increase battery life and improve the technological economy of storage of energy.**

***Index Terms*— Battery, bi-directional DC/DCconverter, HESS, super-capacitor, voltage closed Loop.**

I. INTRODUCTION

With the large amount of renewable energy utilized in the grid, renewable energy power generation (such as solar energy and wind energy) is going to play an indispensable role in the future development of the power system [1]. However, the output power of distributed generation (DG) units are intermittent and random, which brings new challenges to the safe and stable operation of the power system [2, 3]. space, size, weight, changes in transmission, control strategy management etc. Existing on-board Energy storage technology (EST) with the function of "peakcutting and valley filling" is an effective way to solve the power quality of renewable energy generation, and it is also the key technology to ensure the safe and stable operation of the grid [4].The hybrid energy storage system (HESS) has been becoming a hot research topic because it can overcome the limitations of the single energy storage system (ESS) (low power density, low energy density, slow effect speed and short life, etc.) and combine the advantages of both [5]. The ESS is mainly composed of two parts: an energy storage unit and a bi-directional DC/DC converter [6]. A battery ESS can reduce the fluctuation of wind energy output in wind power generation, but the power density of the battery is low [7]. A super-capacitor ESS can realize the storage of regenerative braking energy in urban rail transit, but the low energy density of the super-capacitor may affect the safe and stable operation of the train [8]. An isolated bi-directional DC/DC converter can achieve high power density and current isolation, but when the isolation transformer exists, the leakage inductance and control of the transformer should be considered [9]. Authors of [10] have proposed a high ratio DC/DC converter, which can effectively reduce the voltage stress of the switch. A high-power bi-directional DC/DC converter for distributed photovoltaic power generation has been suggested by [11], which can maximize the solar energy collection capacity.An HESS of a battery and super-capacitor has been presented [12], which effectively combines the advantages of both and reduces the impact of wind energy fluctuation.

However, the HESS is a parallel two independent branches with complex control and poor economy. The application of the HESS in the grid is investigated [13–15]. The results show that the HESS can effectively combine the advantages of a battery and super-capacitor, stabilize the stable operation of the grid and improve the battery life.Based on the study of energy storage requirements for safe and stable operation of a DC microgrid, this paper proposes a battery/super-capacitor HESS, which adopts voltage closed-loop control to improve the voltage stability of a DC bus and the anti-interference performance of the HESS. This paper compares the recovery effect of the HESS and battery ESS on the DC bus voltage to illustrate the advantages of the HESS.

The specific arrangement of the paper is as follows: Section 2 exhibits the topological structure and working principle of the proposed HESS, while section 3 displays the control strategy of the HESS. Section 4 introduces the simulation results and analysis of the system. Finally, section 5 summarizes the article and shows the next work.

II. SYSTEM CONFIGURATION AND WORKING PRINCIPLE

2.1. System configuration

The HESS shares a set of a DC/DC converter, adds a diode D with the function of selective switch, and adds a separate pre-charging circuit as cold stand-by to ensure the normal operation of the super-capacitor. The specific topology is shown in Fig. 1. Among them, UE and UC are the battery and super-capacitor terminal voltages, respectively, and U_d is the DC bus terminal voltage.

2.2. Working modes of the system

The HESS has three working modes: the super-capacitor pre-charging cold stand-by mode, the boost mode and buck mode.

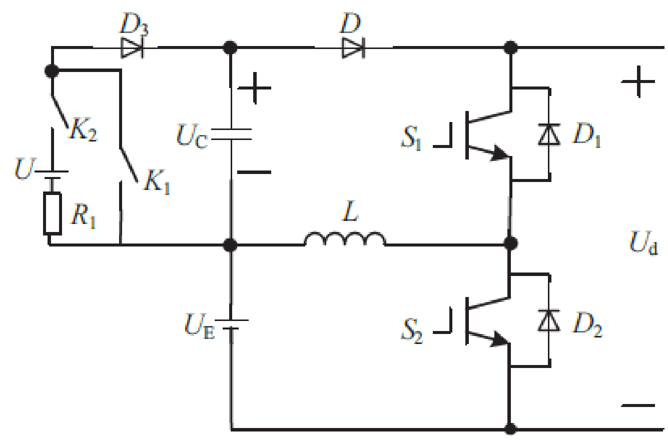

Fig. 1. Structure of battery-super-capacitor HESS

Case 1: the super-capacitor pre-charging cold stand-by mode

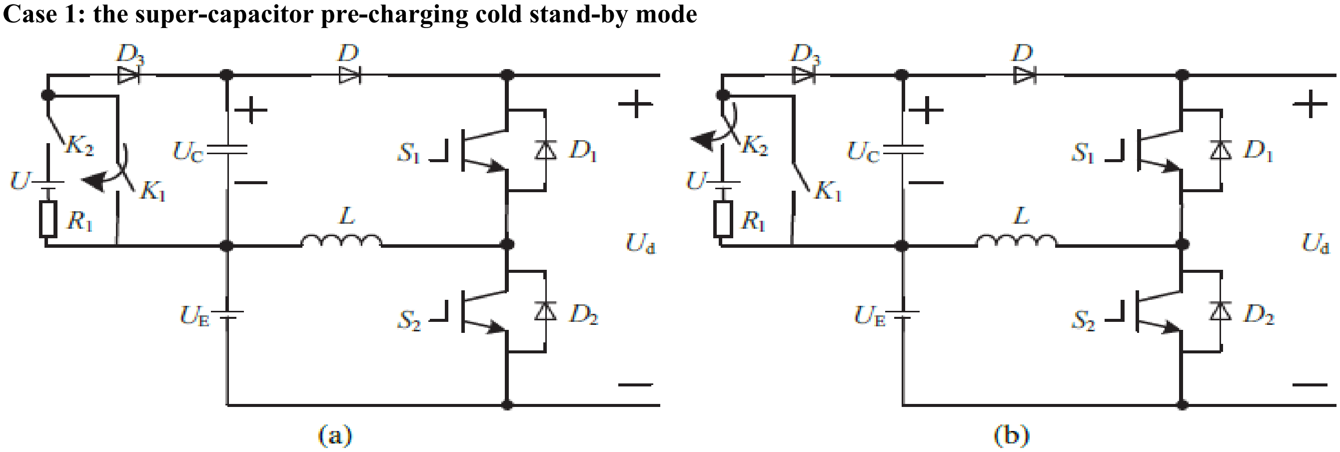

Fig. 2. Equivalent circuit diagram in supercapacitor pre-charging mode:
Working state 1 (a); working state 2 (b)

When the system is in the stand-by state, provided that UC is detected to be in safe working voltage, K1 is closed and K2 is opened. The equivalent circuit diagram is shown in Fig. 2(a). As can be seen from Fig. 2(a), D3 is cut off due to reverse voltage UC, and the super-capacitor pre-charge circuit will not work [16]. Provided that UC is detected to be lower than the cut-off voltage, K1 is opened and K2 is closed. The equivalent circuit diagram is shown in Fig. 2(b). As can be seen from Fig. 2(b), D is cut off due to reverse voltage, and the super-capacitor is in the pre-charge mode.

The super-capacitor pre-charging mode is actually a first-order RC circuit. Power supply U (power supply U is actually introduced from the DC bus voltage to improve the economy of ESS) charges the super-capacitor through discharge resistance R1. Meanwhile, the pre-charge circuit of the proposed topology has been applying the pre-charge of capacitor voltage in the sub-module of the modular multilevel converter.

Case 2: the buck mode

When the DC bus voltage rises, the system operates in the buck mode. Its equivalent circuit diagram is shown in Fig. 3. In buck mode, the anti-parallel diode D2 of switch S2 and switch S1 works alternately.

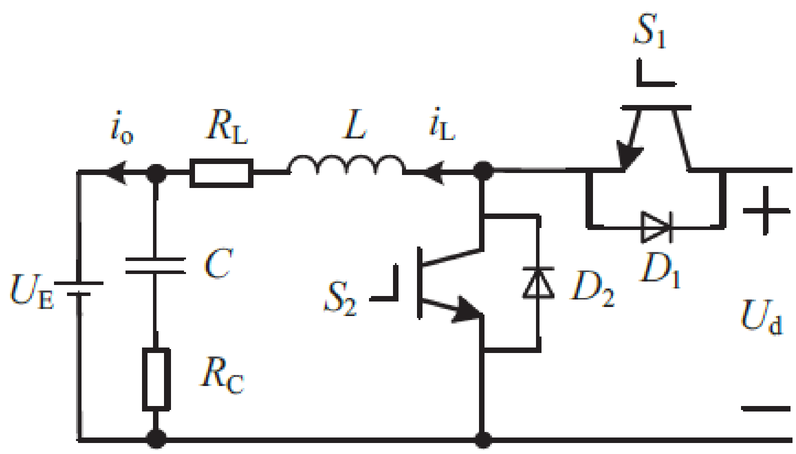

Fig. 3. Equivalent circuit diagram of buck mode

Define switch function *S*:

$$S = \begin{cases} 1 & \text{the } S_1 \text{ or } S_2 \text{ is turned on} \\ 0 & \text{the } S_1 \text{ or } S_2 \text{ is turned off} \end{cases} . \quad (1)$$

According to Fig. 3, the corresponding equation of the state can be obtained as follows:

$$\begin{pmatrix} \frac{di_L}{dt} \\ \frac{du_C}{dt} \end{pmatrix} = \begin{pmatrix} \frac{1}{L} & -\frac{R_L}{L} \\ 0 & \frac{1}{C} \end{pmatrix} \begin{pmatrix} S\,U_d \\ i_L \end{pmatrix} + \begin{pmatrix} -\frac{1}{L} & 0 \\ 0 & -\frac{1}{C} \end{pmatrix} \begin{pmatrix} U_E \\ i_o \end{pmatrix} . \quad (2)$$

According to Equation (2) and the state space average method [17], the corresponding average equation can be obtained:

$$\begin{pmatrix} \frac{di_L}{dt} \\ \frac{du_C}{dt} \end{pmatrix} = \begin{pmatrix} \frac{D}{L} & -\frac{R_L}{L} \\ 0 & \frac{1}{C} \end{pmatrix} \begin{pmatrix} U_d \\ i_L \end{pmatrix} + \begin{pmatrix} -\frac{1}{L} & 0 \\ 0 & -\frac{1}{C} \end{pmatrix} \begin{pmatrix} U_E \\ i_o \end{pmatrix}, \tag{3}$$

Where:

$D = t_{on}/(t_{on} + t_{off})$, is the duty cycle of S_1.

Added disturbance:

$$\begin{cases} d = D + \hat{d} \\ i_L = I_L + \hat{i}_L \\ u_d = U_d + \hat{u}_d \\ u_E = U_E + \hat{u}_E \\ u_C = U_C + \hat{u}_C \end{cases} . \tag{4}$$

By substituting Formula (3), the small signal transfer function of control-voltage can be obtained through the Laplace transformation:

$$G_{vd1} = \left. \frac{\hat{u}_E(s)}{\hat{d}(s)} \right|_{\hat{u}_d(s)=0} = \frac{U_d(s)}{LCs^2 + R_L Cs + 1} . \tag{5}$$

Case 3: the boost mode

When the DC bus voltage decreases, the system operates in the boost mode. Its equivalent circuit diagram is shown in Fig. 4. In the boost mode, the anti-parallel diode D1 of switch S1 and switch S2 works alternately.

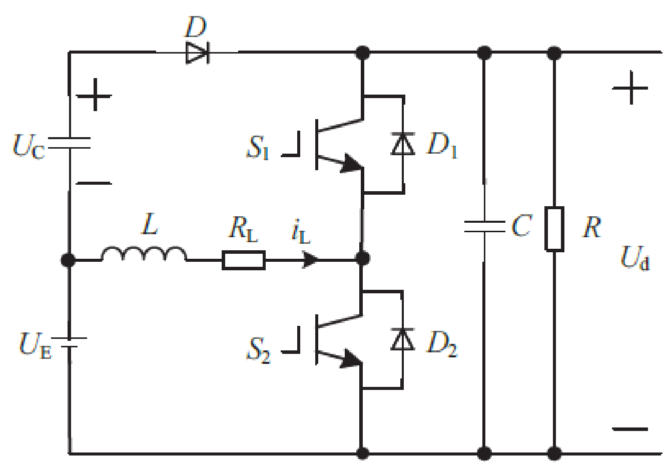

Fig. 4. Equivalent circuit diagram of boost mode

According to Fig. 4, the corresponding equation of the state can be obtained as follows:

$$\begin{pmatrix} \frac{\mathrm{d}i_{\mathrm{L}}}{\mathrm{d}t} \\ \frac{\mathrm{d}u_{\mathrm{d}}}{\mathrm{d}t} \end{pmatrix} = \begin{pmatrix} -\frac{(1-S)}{L} & -\frac{R_{\mathrm{L}}}{L} \\ -\frac{1}{RC} & \frac{(1-S)}{C} \end{pmatrix} \begin{pmatrix} U_{\mathrm{d}} \\ i_{\mathrm{L}} \end{pmatrix} + \begin{pmatrix} \frac{1}{L} \\ 0 \end{pmatrix} U_{\mathrm{E}}. \quad (6)$$

According to Equation (6) and the state space average method, the corresponding average equation can be obtained:

$$\begin{pmatrix} \frac{\mathrm{d}i_{\mathrm{L}}}{\mathrm{d}t} \\ \frac{\mathrm{d}u_{\mathrm{d}}}{\mathrm{d}t} \end{pmatrix} = \begin{pmatrix} -\frac{(1-D)}{L} & -\frac{R_{\mathrm{L}}}{L} \\ -\frac{1}{RC} & \frac{(1-D)}{C} \end{pmatrix} \begin{pmatrix} U_{\mathrm{d}} \\ i_{\mathrm{L}} \end{pmatrix} + \begin{pmatrix} \frac{1}{L} \\ 0 \end{pmatrix} U_{\mathrm{E}}, \quad (7)$$

Where:

$D = t_{\mathrm{on}}/(t_{\mathrm{on}} + t_{\mathrm{off}})$, is the duty cycle of S_2.

By substituting Formula (4) into Formula (7), the small signal transfer function of control- voltage can be obtained through the Laplace transformation.

$$G_{vd2} = \left.\frac{\hat{u}_{\mathrm{d}}(s)}{\hat{d}(s)}\right|_{\hat{u}_{\mathrm{d}}(s)=0} = \frac{U_{\mathrm{d}}(s)\left(D' - \frac{R_{\mathrm{L}} + sL}{RD'}\right)}{LCs^2 + \left(R_{\mathrm{L}}C + \frac{L}{R}\right)s + \frac{R_{\mathrm{L}}}{R} + D'}, \quad (8)$$

where: $D' = 1-D$

3. CONTROL STRATEGY

The energy management of the HESS mainly depends on the control strategy of a bi-directional DC/DC converter, that is, the charge and discharge of a battery and super-capacitor bank are realized by controlling the bi-directional DC/DC converter. It is the core of control to keep the voltage of the DC bus constant. In this paper, the voltage closed-loop control is used to make the DC bus voltage stable at the rated voltage quickly. The way to generate the control pulse of the bi-directional DC/DC converter is mainly composed of complementary pulse width modulation (PWM) and independent PWM. The difference between them is whether the driving signals of S1 and S2 are complementary. In order to improve the stability of the system, the independent PWM mode is used.

The bi-directional DC/DC converter control strategy of the HESS consists of two parts: a logic judgment unit and a voltage closed-loop control unit. The specific control block diagram is shown in Fig. 5. When the voltage U_d suddenly rises (such as locomotive braking process), the difference ΔUd1 between the reference voltage U^*_d at the DC bus and the actual value Ud, then the theoretical duty cycle d'_1 is obtained through PI and the limiting link, and then the current actual duty ratio d1 is obtained by combining the independent PWM mode. At this time, the HESS works in the buck mode, S2 is off, S1 is in PWM. When the voltage U_d suddenly drops (such as the starting process of the locomotive), the difference ΔUd_2 between the reference voltage U^*_d at the DC bus and the actual value U_d, then the theoretical duty cycle d'_2 is obtained through the proportional-integral (PI) and limiting link, and then the current actual duty ratio d_2 is obtained by combining the independent PWM mode. At this time, the HESS works in the boost mode, S1 is off, S2 is in the PWM. The PI is used to realize the tracking control of U_d at the DC bus to U_d ref.

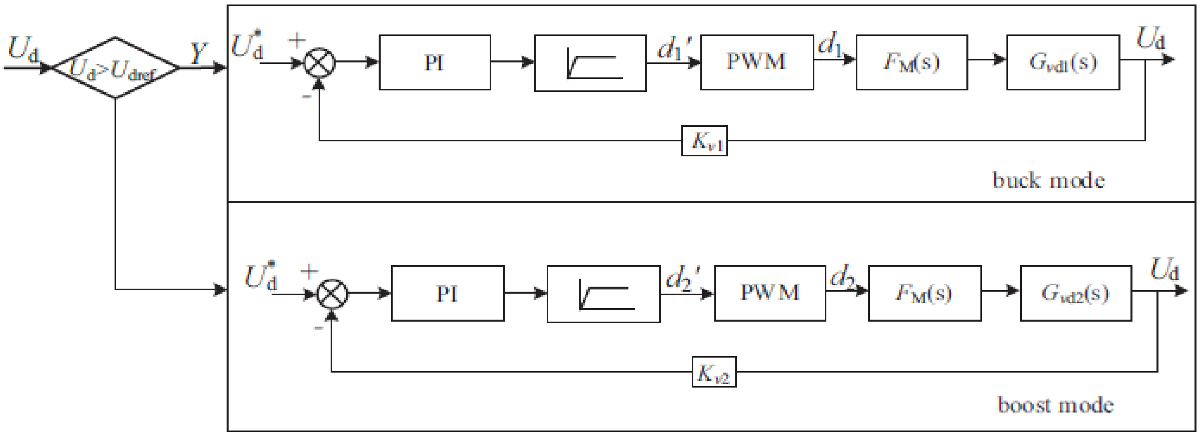

Fig. 5. Control strategy block diagram of bi-directional DC/DC converter for HESS

3.1. Simulation results and discussion

In order to verify the effectiveness of the HESS and its control strategy, Matlab/Simulink scientific computing environment was used to simulate, and the main simulation parameters of the system are shown in Table 1. Fig. 6 shows the pre-charge waveform of the super-capacitor when the discharge depth of the super-capacitor is 50%. From Fig. 6, it can be seen that when the super-capacitor voltage is detected to be reduced to 24 V or below, the super-capacitor pre-charging circuit is activated to Charge the super-capacitor. At 600 ms, the super-capacitor voltage reaches 47.2 V, and the power supply will be restored to the normal working voltage. Meanwhile, the pre-charge time of the super-capacitor is within a reasonable range [18].

Table 1. Main simulation parameters of the system

Parameter name	Symbol	Value	Unit
Battery voltage	U_E	48	V
Super-capacitor voltage	U_C	48	V
DC bus voltage	U_d	120	V
Inductance	L	8.2×10^{-5}	H
Discharge resistance	R_1	6.94×10^{-5}	Ω
Output capacitance	C	3.76	mF

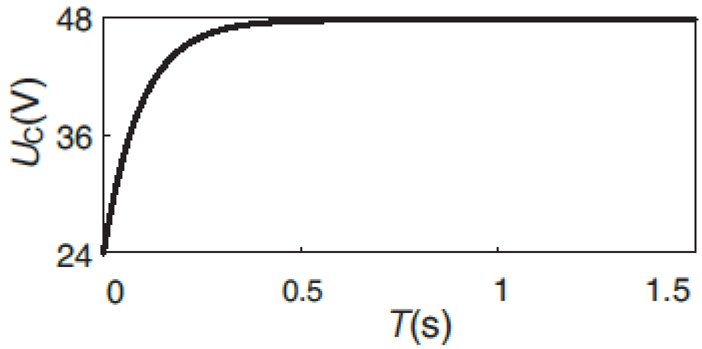

Fig. 6. Pre-charging waveform of super-capacitor

Case 1: no load disturbance

When the DC bus voltage suddenly decreases (such as the moment of motor start, etc.), the system works in the boost mode. Fig. 7 shows the waveform of the DC bus voltage *U*d of the HESS and the battery ESS in the boost mode when the DC bus voltage is reduced to 90 V. It can be seen from Fig. 7 that under the HESS, the maximum voltage *U*d at the DC bus is 134.1 V, and the *U*d stability value is 120 V; the system overshoot is about 11.6%; the system regulation time is 0.95 ms; the voltage ripple is about 0.73%, less than 2%. Under the battery ESS, the stable value of the DC bus voltage *U*d is 123.9 V, the stable value of *U*d is 119.8 V; the system overshoot is about 3.5%; the system regulation time is 1.45 ms. The regulation time of the battery ESS is 34.5% longer than that of the HESS. Therefore, the DC bus voltage recovery effect and dynamic
Performance of the HESS in the boost mode are better than that of the battery ESS.

When the DC bus voltage suddenly increases (such as locomotive braking process, etc.), the system works in the buck mode. Fig. 8 shows the waveform of the DC bus voltage Ud in the buck= mode when the DC bus voltage increases by 150 V. It can be seen from Fig. 8 that under this condition, the stable value of the DC bus voltage Ud is 118.55 V; the system overshoot is about 11.25%; the system regulation time is 0.8 ms; the voltage ripple is about 0.75%, less than 2%.

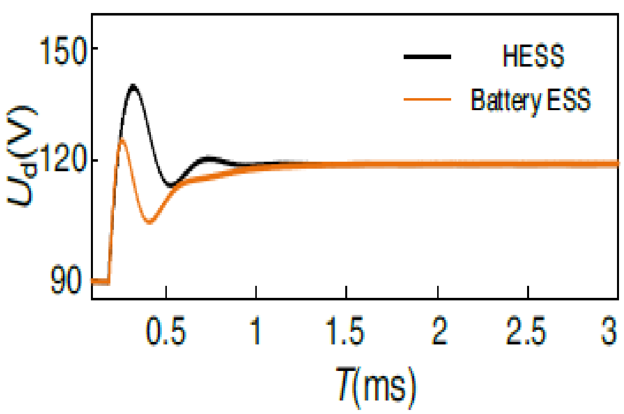

Fig. 7. Waveform of boost mode

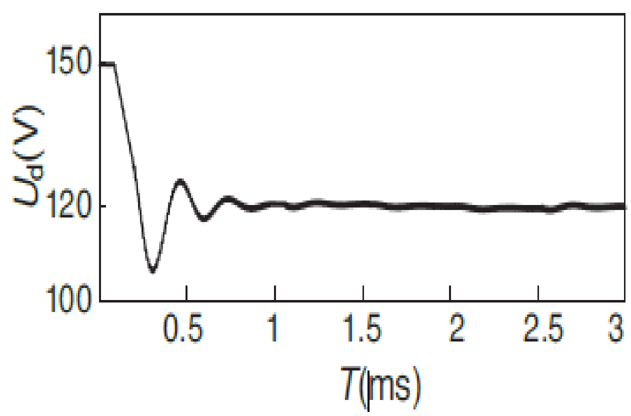

Fig. 8. Waveform of buck mode

Case 2: adding load disturbance

When the DC bus voltage suddenly decreases (such as the moment of motor start, etc.), the system works in the boost mode. A periodic load disturbance is added at 1 ms to decrease the DC bus voltage, and a periodic load disturbance is added at 2 ms to increase the DC bus voltage. Fig. 9 shows the waveform of the voltage Ud at the DC bus of the proposed HESS in the boost Mode when the load disturbance is added. It can be seen from Fig. 9 that the voltage at the DC bus drops to 111.8 V in 1 ms and recovers to 120 V after 0.305 ms; the voltage at the DC bus rises to 129.5 V in 2 ms and recovers to 120 V after 0.385 ms. When the DC bus voltage suddenly increases (such as locomotive braking process, etc.), the system works in buck mode. A periodic load disturbance is added at 1 ms to decrease the DC bus voltage, and a periodic load disturbance is added at 2 ms to increase the DC bus voltage. Fig. 10 shows the waveform of the DC bus voltage Ud in buck mode of the proposed HESS when the load disturbance is added. It can be seen from Fig. 10 that the voltage at the DC bus drops to 114.3 V in 1 ms and recovers to 119.8 V after 0.41 ms; the voltage at the DC bus side rises to 126.3 V in 2 ms and recovers to 119.8 V after 0.39 ms.

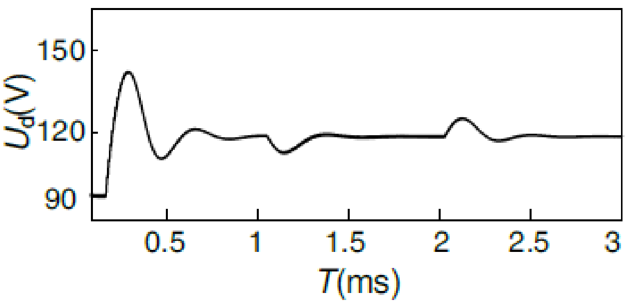

Fig. 9. Waveform of boost mode with load disturbance

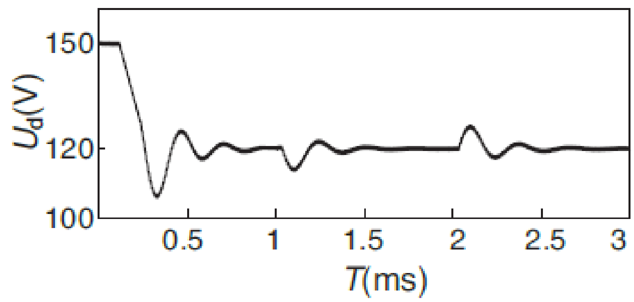

Fig. 10. Waveform of buck mode with load disturbance

4. CONCLUSION

Maintaining a constant DC bus voltage is the first prerequisite for the safe and stable operation of the DC micro grid. In this paper, the HESS and its control strategy are analysed in theory and simulation. The results demonstrate that the HESS and its control strategy can increase the service life of the battery, reduce the size of the battery, and improve the economy of the ESS. Simultaneously, the super-capacitor pre-charge cold standby state and the boost, buck mode work

Independently. The diode D with the function of a selective switch can charge the main power battery, and the super-capacitor pre-charge circuit, as the cold standby, effectively guarantees the performance of the super-capacitor. In addition, the voltage ripple of the HESS and its control strategy is small, while the voltage stabilizing effect and the anti-interference performance is superior.

Finally, the next step is to verify the proposed HESS in practical engineering, and further discuss and analyze the coordinated control strategy of the HESS for a micro grid.

5. REFERENCES

[1] Telukunta V., Pradhan J., Agrawal A., Singh M., Srivani S.G., Protection challenges under bulk penetration of renewable energy resources in power systems: A review, CSEE Journal of Power and Energy Systems, vol. 3, no. 4, pp. 365–379 (2017), DOI: 10.17775/CSEEJPES.2017.00030.

[2] Zhang C., Chen H., Liang Z., MoW., Zheng X., Hua D., Interval voltage control method for transmission systems considering interval uncertainties of renewable power generation and load demand, IET Generation, Transmission and Distribution, vol. 12, no. 17, pp. 4016–4025 (2018), DOI: 10.1049/iet- gtd.2018.5419.

[3] Fan M., Sun K., Lane D., Gu W., Li Z., Zhang F., A Novel Generation Rescheduling Algorithm to Improve Power System Reliability with High Renewable Energy Penetration, IEEE Transactions on Power Systems, vol. 33, no. 3, pp. 3349–3357 (2018), DOI: 10.1109/TPWRS.2018.2810642.

[4] Zhang Z., Zhang Y., Huang Q., Lee W., Market-oriented optimal dispatching strategy for a wind farm with a multiple stage hybrid energy storage system, CSEE Journal of Power and Energy Systems, vol. 4, no. 4, pp. 417–424 (2018), DOI: 10.17775/CSEEJPES.2018.00130.

[5] YanN., Zhang B., LiW.,MaS., Hybrid Energy Storage Capacity Allocation Method for Active Distribution Network Considering Demand Side Response, IEEE Transactions on Applied Superconductivity, vol. 29, no. 2, pp. 1–4 (2019), DOI: 10.1109/TASC.2018.2889860.

[6] Jiang W., Zhu C., Yang C., Zhang L., Xue S., Chen W., The Active Power Control of Cascaded Multilevel Converter Based Hybrid Energy Storage System, IEEE Transactions on Power Electronics, vol. 34, no. 8, pp. 8241–8253 (2019), DOI: 10.1109/TPEL.2018.2882450.

[7] Zhang Y., Iu H.H., Fernando T., Yao F., Emami K., Cooperative Dispatch of BESS and Wind Power Generation Considering Carbon Emission Limitation in Australia, IEEE Transactions on Industrial Informatics, vol. 11, no. 6, pp. 1313–1323 (2015), DOI: 10.1109/TII.2015.2479577.

[8] Yang Z., Yang Z., Xia H., Lin F., Brake Voltage Following Control of Supercapacitor-Based Energy Storage Systems in Metro Considering Train Operation State, IEEE Transactions on Industrial Electronics, vol. 65, no. 8, pp. 6751–6761 (2018), DOI: 10.1109/TIE.2018.2793184.

[9] He P., Khaligh A., Comprehensive analyses and comparison of 1 kW isolated DC-DC converters for bidirectional EV charging systems, IEEE Transactions on Transportation Electrification, vol. 3, no. 1, pp. 147–156 (2017).

[10] Kim K., Cha H., Park S., Lee I., A Modified Series-Capacitor High Conversion Ratio DC–DC Converter Eliminating Start-Up Voltage Stress Problem, IEEE Transactions on Power Electronics, vol. 33, no. 1, pp. 8–12 (2018), DOI: 10.1109/TPEL.2017.2705705.

[11] Suntio T., Kuperman A., Comments on An Efficient Partial Power Processing DC/DC Converter for Distributed PV Architectures, IEEE Transactions on Power Electronics, vol. 30, no. 4, pp. 2372–2372 (2015), DOI: 10.1109/TPEL.2014.2327018.

[12] Wang J., Xu Y., Lv M., Modeling and simulation analysis of hybrid energy storage system based on wind power generation system, IEEE:2018 International Conference on Control, Automation and Information Sciences (ICCAIS), Hangzhou, China, pp. 422–427 (2018).

[13] Bahloul M., Khadem S.K., Impact of Power Sharing Method on Battery Life Extension in HESS for Grid Ancillary Services, IEEE Transactions on Energy Conversion, vol. 34, no. 3, pp. 1317–1327 (2019), DOI: 10.1109/TEC.2018.2886609.

[14] Xiao J., Wang P., Setyawan L., Multilevel Energy Management System for Hybridization of Energy Storages in DC Micro grids, IEEE Transactions on Smart Grid, vol. 7, no. 2, pp. 847–856 (2016), DOI: 10.1109/TSG.2015.2424983.

[15] Ma W., Optimal Allocation of Hybrid Energy Storage Systems for Smoothing Photovoltaic Power Fluctuations Considering the Active Power Curtailment of Photovoltaic, IEEE Access, vol. 7, pp. 74787–74799 (2019), DOI: 10.1109/ACCESS.2019.2921316.

[16] Li B.B., Xu D.D., Zhang Y., Yang R.F., Wang G.L., Xu D.G., Closed-loop pre-charge control of modular multilevel converters during start-up processes, IEEE Transactions on Power Electronics, vol. 30, no. 2, pp. 524–531 (2015), DOI: 10.1109/TPEL.2014.2334055.

[17] Wang L., Electromagnetic Transient Modeling and Simulation of Power Converters Based on a Piece- wise Generalized State Space Averaging Method, IEEE Access, vol. 7, pp. 12241–12251 (2019), DOI: 10.1109/ACCESS.2019.2891122.

[18] Chen P.P.,Wang X.Q., Design of Pre-charge Resistor Selection for Power Battery, Bus and Coach Technology and Research, vol. 40, no. 01, pp. 30–33 (2018), DOI: 10.15917/j.cnki.1006-3331.2018.01.009.